Iraq University College Journal of Engineering and Applied Sciences

Physicochemical Properties of Short Sisal Fibers-Ethylene Vinyl Acetate Composites following Fiber Surface Treatments

Madera-Santana T. J[1,a], Soto Valdez .H[1,a] , Richardson M.O.W[2,b] ,Alhassani A. H[3,c,*]

1 Senior Researchers, Laboratorio de Envases. CTAOV. Centro de Investigación en Alimentosy Desarrollo, A.C. Km. 0.6 Carr. a La Victoria. A.P. 1735. 83304 Hermosillo, Sonora. México .
2 Professor Emeritus, School of Engineering, University of Portsmouth, Anglesea Building, Anglesea Road. Portsmouth, Hampshire PO1 3DJ. U.K.
3 Communication Engineering Dep., Iraq University College, Basrah - Iraq.
E-mail: alhassani@yahoo.com

Abstract. Natural fibers (NF) are a cheap, easily renewable resource for cellulose-rich polymer composites. Impurities (waxes, lignin, etc.) and hydroxyl groups, on the other hand, decrease the likelihood of NF reinforcing polymeric matrices. Three different chemical treatments were applied to short sisal fibers (SSF) (dicumyl peroxide, alkaline and silane). Mechanical mixing at the melt stage of the polymer matrix (130° C) was employed to create composites of ethylene vinyl acetate (EVA) and chemically modified SSF.The mechanical properties of biocomposites were studied in relation to fiber content and chemical treatment. Every SSF reinforced composite that had been treated had a higher tensile strength. The elastic modulus compound increased significantly when compared to the empty matrix. As the fiber content was raised, the elongation at break values fell. Furthermore, it was discovered that the SSF's surface treatment increased fiber dispersion within the EVA matrix. The thermogravimetic analysis (TGA) was used to examine SSF's thermal stability . Because natural fiber has a lower specific gravity, it is less expensive and has the added benefit of biodegradability and the composites' recyclability .

Keywords: Natural fibers, short sisal fibers, ethylene vinyl acetate, thermogravimetic analysis.

Iraq University College Journal of Engineering and Applied Sciences Volume 2, Issue 1
Received 04/03/2022
Accepted 13/04/2022
Published 27/06/2022
Online at https://magazine.iuc.edu.iq/journal/ ISSN 2790-704X; 2790-7058
DOI:yy.yyyy/ IUCJEAS. 2022.xx.x.xx

1. Introduction

Composites of hard or stiff natural fibers in soft matrices can be made out of natural rubber (NR), styrene-butadiene rubber (SBR), low density polyethylene (LDPE), ethylene vinyl acetate (EVA), and other soft matrices [1-3]. The economic aspect is important since composite enterprises require a lower cost for fiber component manufacture while simultaneously improving quality. Natural fibers are one way to accomplish this. Natural fibers provide a number of advantages over conventional inorganic fibers, including low price and width, high specific strength and modulus, renewable resources, and ease of processing [4-6]. Due to the presence of hydroxyl groups, natural fibers (such as jute, henequen, hemp, sisal, and others) are extremely polar. However, pectin and waxy substances coat these fibers, preventing the hydroxyl groups from interacting with polar matrices and producing mechanical interlocking adhesion with non-polar matrices [7]. Natural fibers can be treated to physically or chemically to modify their surface and plan in order to deliver responsive hydroxyl groups and a rough surface for adhesion with polymeric matrices [8-9].

Many studies on natural fiber composites with thermoplastic matrices (PMMA, HDPE, PP, LDPE, PS, etc.) have been published in the last two decades, and composites with treated natural fibers and additionally altered matrix have shown to have better properties than composites with non-modified fibers and matrix [5-10]. Common processing techniques like as bambury and expulsion can be used to create natural fiber composites in polymeric matrices. In most cases, discontinuous short fibers are incorporated into a molten thermoplastic matrix, and the fibers are normally oriented randomly within the matrix. A variety of issues plague thermoplastic-natural fiber composites,, including inferior compatibility with the hydrophobic polymeric matrix, a propensity to make agglomerates during manufacturing, and low watertight tendency. [10-11]. Furthermore, numerous parameters influence the properties of thermoplastic composites made with short fibers, including fiber-matrix adhesion, fiber concentration (fiber volume fraction), fiber aspect ratio, fiber orientation, and interface stress transmission efficiency [12-13]. Chemical compatibility is one criterion for optimal bonding between natural fibers or fillers in a thermoplastic matrix. However, this connection makes dispersing the fibers in a hydrophobic matrix problematic. According to Georpoulos et al [11], natural fibers are difficult to disperse in non-polar polymers during processing due to their significant intermolecular hydrogen bonding. As a result, dispersion agents such as stearic acid, solid paraffin wax, or natural oil must be utilized [14-15]. Natural fibers are typically treated on the surface to flat on their similarity with the matrix. Because of their hydrophilic nature, cellulose fibers are often believed to be incompatible with hydrocarbon polymers; however, many treatments have been observed to increase fiber-matrix interfacial interaction. Mwaikambo and Ansell [7], Joseph et al. [16], and Alvarez Vera and Vazquez [17] all reported on the physical and mechanical properties of thermoplastic composites produced with alkaline-treated sisal fibers. Chemical treatments such as isocyanate treatment, acrylation, and permanganate treatment, as well as the use of coupling agents like peroxides, silanes, titanates, and isocyanates on natural fibers (jute, coir, cellulose, and sisal) have been reported in the literature to improve fiber adhesion, processability, and mechanical properties [6,14,18]. In this case, a simple surface treatment can be applied to the fibers during the cleaning process to change the surface and increase surface roughness [19].

EVA copolymer is utilized in a variety of applications, including wire and cable insulation, barrier sheets, adhesives and paper coatings, and packaging films [20]. The characteristics of EVA-natural fiber composites, on the other hand, have received less attention. Dikobe and Luyt studied PP/EVA composites with wood powder (WP) and found that WP altered EVA crystallization behavior [21]. Mydul et al. [22] evaluated mechanical characteristics of EVA and cellulose acetate (CA) containing natural fibers (Sterculia villosa). They discovered that the tensile strength of EVA composites declined as fiber was added, whereas the tensile strength of CA composites rose due to the well-distributed fibers. Uncrosslinked and crosslinked EVA-sisal fiber composites were reported by Malunka et al [23], and dicumyl peroxide (DCP) was found to be successful in grafting EVA to sisal fiber; composites with crosslinked EVA had better characteristics and thermal stability than uncrosslinked composites. Water absorption resistance of

natural fiber composites can be enhanced; Espert et al. investigated PPEVA-cellulose fiber composites and found that EVA reduced water absorption [24].

Short sisal fibers (SSF) were treated to three distinct chemical treatments in this investigation (alkaline, dicumyl peroxide and silane). SSF that had been chemically changed were integrated into an EVA copolymer matrix. The chemical change of SSF by three distinct treatments was investigated using FTIR. As a function of fiber weight fraction and fiber treatment, mechanical parameters (tensile strength, elongation at break, and tensile modulus) were investigated. The fiber surface modification and fibermatrix adhesion were evaluated using scanning electron microscopy (SEM).

2. Experimental

2.1 Materials

Local Yucatán sources provided sisal fibers (agave-sisalana), which were chopped and processed. The average fiber diameter and fiber length were 210 m and 5.5 mm, respectively, according to aspect ratio measurements. Short sisal fibers (SSF) were completely washed with water and dried for 6 hours in a convection air oven at 90°C. Elf Atochem, UK Ltd. provided the ethylene-vinyl acetate (EVA) copolymer (EVATENE). The vinyl percentage of this EVA copolymer is 18%. The physical and mechanical parameters of the materials utilized are listed in Table 1.

Fisher Scientific UK provided 95 percent methyl alcohol and sodium hydroxide (NaOH). Aldrich Chemical Corp. provided the dicumyl peroxide (DCP) and potassium bromide (KBr) FTIR grades. Accros Organics Ltd provided N-[3-(trimethoxysilyl) propyl]-ethylene diamine (as a silane coupling agent). All of the reactants utilized in this experiment were chemically pure.

2.2 Chemical Treatments

The sisal fibers were given three distinct surface treatments in order to improve fiber-matrix adhesion. The first was mercerization [25], an alkali treatment. The surface topology of sisal fiber was altered, resulting in a rough surface. The second experiment involves using a reactive system to generate free radicals on the fiber surface. A silane coupling agent was utilized in the third procedure to build a bridge (covalent bonds) between the fiber and the matrix.

Alkaline Treatment. SSF were placed in a 4 L glass baker, then a solution of NaOH (10% wt) was added and mechanically agitated for 1 hour at 70 rpm. The fiber weight to alkali solution volume ratio was 1:20. The fibers were then thoroughly rinsed with water to eliminate any excess NaOH. The final wash was done with distilled water and 1% acetic acid by volume. The fibers were then dried overnight at 60°C in a convection air oven.

Dicumyl peroxide (DCP) Treatment. SSF were soaked in 1 L of a 6 percent v/v DCP in acetone for 30 minutes before being alkaline treated. The solution was decanted, and the fibers were dried overnight at 60°C in a convection oven.

Silane Treatment. SSF that had previously been alkaline treated were placed in a glass kettle reactor with a methanol/water (90 percent v/v) solution at a pH of roughly 3.5 (25C). The silane content in the solution was 1% by volume. The fibers were decanted and dried in a convection air oven at 60°C overnight after 1 hour of gentle stirring.

2.3 Fiber Characterization by FTIR and TGA

To evaluate the chemical changes in/on the fibers, an IR spectrum was taken after each chemical treatment. The samples were thoroughly mixed with 200 mg of dry KBr in a mortar. The FTIR spectra were collected in a single beam mode with a resolution of 2 cm-1 in the frequency range of 4000-400 cm-1 using a Nicolet Protege 460 Fourier Transform spectrophotometer. Averaging 100 scans of the signal produced each spectrum.

Thermogravimetric analyses (TGA) of untreated and treated SSF were performed using a Perkin Elmer TGA-7 thermogravimetric analyzer from room temperature to 600oC at a heating rate of 10oC/min in nitrogen environment. Composites Preparation and Characterization. In a laboratory scale two roll mill supplied by England Co. Ltd., untreated and treated short sisal fibers were mixed with EVA copolymer at varying weight percentages of 10, 20, 30, and 40% wt. To achieve total dispersion, the mill was set to 120°C oil bath temperature and the mixing was done for 10 minutes at a roll speed of 50 rpm. Compression molding at 120°C and 100 psi between steel plates produced 1.5 mm thick samples for mechanical tests. Tensile tests were conducted at room temperature in a J.J. Lloyds tensile testing machine (2000R) with dumbbell-shaped specimens (following ASTM D-38 method). The crosshead speed was set to 50 millimeters per minute. A Cambridge Stereo-Scan (Model S-360) scanning electron microscope was used to analyze the cracked surfaces of the EVA biocomposites with 30% SSF at various magnifications. To eliminate electrostatic charge during examination, the broken specimens were mounted on aluminum stubs and sputtered with a small layer of gold to get some information regarding the bonding quality between the fiber and matrix, as well as the fiber dispersion.

2.4 Statistical analysis

The data was examined using a two-sample t-student test. ANOVA test ($p<0.05$) was used to examine the effect of chemical treatment and fiber content on mechanical characteristics. Statistical software was used to determine all of these statistical processes (Statistica, Statsoft Inc.).

3. Results and Discussion

3.1 Characterization of Chemically Modified SSF by FTIR

Due to the presence of hydroxyl groups, which are involved in hydrogen bonding inside cellulose molecules, SSF are vulnerable to chemical alteration. By activating these groups, factors that constitute effective interlocks within the system can be introduced. Surface properties of SSF are improved via chemical treatment (wetting, adhesion, surface tension, porosity, etc.) [3,6]. The IR spectra of untreated and treated SSF at two different wavenumber areas are shown in Figures 1(a) and 1(b). Alkali treatment affects the bands 3380, 2900, 1738, 1420, 1375, 1320, 1240, and 895 cm^{-1}. Untreated SSF displays a characteristic O-H stretching band at 3380 cm^{-1}, which corresponds to hydroxyl groups on anhydrogalactose bonds; however, upon alkali treatment, this band decreased. This is due to the elimination of – OH groups by sodium hydroxide reaction. Because they were likewise subjected to alkaline treatment, SSF with DCP and silane treatments showed similar characteristics. After chemical treatment, the C-H vibration band at 2900 cm^{-1}due to methyl and methylene bonds shifts to 2880 cm^{-1}, as seen in Fig. 1(a). This band is linked to the lignin – OCH_3 bonds and the silane coupling agent's CH_2 groups. The peak at 1740-1735 cm^{-1} found in untreated SSF (Fig 1b) fades away after DCP and silane treatment, but not with alkaline treatment. Deesterification [7] is the process of removing this band, which corresponds to a carboxylic group. The peak vanishes when large amounts of waxes and uronic acid (a component of hemicellulose and xylene) are eliminated. Furthermore, this treatment has been shown to increase crystallinity while decreasing fiber sorption capacity [7-26]. The peak height ratio of the >C=O band at 1740-1735 cm^{-1} to the peak of the CH_2 stretching band at 1514 cm^{-1}, which is classified as an internal standard band, was used to compute the absorption intensities of the C=O group because it did not vary with the chemical treatments. This study revealed a decrease in overall ester content and the strength of the >C=O band. In addition, SSF treated with silane

exhibits an increase in peak intensity at 1645 and 1555 cm^{-1}, indicating a partial reaction of hemicellulose C=O linkages with silane complex and amine production, respectively. As a result, the alkaline treatment did not remove all of the hemicellulose from the SSF, potentially allowing more reactive sites for DCP and the silane coupling agent.

The crystalline area, exhibited in Fig. 1(b), was enlarged by the alkaline treatment, with peaks at 1400-1300 cm^{-1}. Because of the alkali and silane treatment, the intensity of the COO- group band at 1420 cm^{-1} is somewhat elevated. Measurement of the absorption ratio (1372/2900 cm^{-1}) has been advocated by certain writers, such as Nelson and O'Connors [27], as a way of assessing how the crystallinity index declines with increasing alkali strength during mercerization. Reddy [28] suggested that the optimal absorption band for this purpose is 880 cm^{-1} in one investigation. Oh et al. [29] recently claimed that the relative absorbance ratio $A_{(4000-2995)}/A_{1337}$ shows the decrease of absorbance as a hydrogen bond intensity requirement (HBI). The degree of intermolecular regularity (crystallinity) and the amount of bound water affect the HBI of SSF. As an empirical determination of HBI, the ratio $A_{(4000-2995)}/A_{1337}$ was introduced [29]. Table 2 demonstrates that treated SSF has a lower absorbance ratio at 4000-2995 and 1337 cm^{-1}. This means that the chemical treatments changed the cellulose crystal structure in SSF from cellulose I to cellulose II, which is thermodynamically more stable than cellulose I. Because chemical treatments enhance the absorbance at 900 cm^{-1}, the absorbance ratio 11 of bands at 1430 and 900 cm^{-1} A_{1430}/A_{900} is used as the crystallinity index (CI), which is proportional to the proportion of cellulose I structure.

In alkali treated fibers, however, the band at 1240 cm^{-1} (assigned to the C-O stretching mode of the COO- group of hemicellulose) is shifted to 1248 cm-1, despite the appearance of two medium bands at 1260 and 1225 cm^{-1} in silane treated fibers, which could be due to C-O and O-H bending, respectively. The 900 cm^{-1} band is due to antisymmetrical stretching of the C_1-O-C_4 β-glucosidic linkage (in the C-H frequency) and unreacted silanol groups (Si-O stretching) formed during hydrolysis. As a result, a shift in the intensity of this band indicates a change in cellulose structure. The existence of a peak at 1630 cm^{-1} after silane treatment on SSF can be explained by the amine production band. The appearance of two minor absorption bands at 763 and 703 cm^{-1} corresponds to the symmetric stretching of -Si-C- and -Si-O-Si-, respectively [30]. The presence of polysiloxanes deposited on the fiber is shown by the –Si-C- bond, which confirms the occurrence of a condensation reaction between the silane coupling agent and SSF.

3.2 Thermal analysis

The low thermal resistance of some natural fibers precludes the use of an arbitrary thermoplastic matrix. It is critical to understand the thermal degradation of natural fiber composites while processing them since they may be exposed to high processing temperatures for extended periods of time. Figure 2(a) depicts the thermal degradation of the fibers with and without treatment, while Figure 2(b) depicts the thermograms' first derivative. The thermal analysis of treated SSF revealed that these 12 thermograms varied from the thermogram of untreated SSF. Near 100°C, all thermograms show a modest decrease of mass, which is due to the loss of surface water (moisture) in the fibers. It's worth noting that the thermal stability of the untreated and treated SSF is maintained until 280°C, with no mass loss or degradation occurring between 120 and 270°C. Untreated SSF decomposes in two steps above this temperature. In an inert atmosphere, the initial breakdown shows a little shoulder, which is commonly attributed to heat depolymerization of hemicelluloses and breakage of glucosidic links of cellulose [31]. The degradation of -cellulose causes the second step at 382°C; comparable results have been found in fique fibers [32] and other natural fibers [31]. Because all substances (waxes, hemicelluloses, tamo, etc.) were eliminated by surface treatments, the treated fibers only show the second degradation step. On the other hand, the decomposition temperature in each treatment is slightly different, as seen in the first derivative curves. This could be due to a chemical reaction that occurs between the fiber and the chemicals used in treatment. Because the amorphous phase has been removed and the cellulose functional groups have been fixed, SSF is likely to have a better crystal structure.

3.3 Morphological aspect of sisal fibers

Sisal fiber is a type of ligno-cellulosic fiber classed as a hard natural fiber [25]. Chemical treatments change the topology of the fiber by removing surface contaminants, waxes, and oil terpenic agents, among other things. A microphotograph of the surface of untreated sisal fiber, shown in Fig. 3(a), reveals knots of dust, waxes, and other contaminants. The surface morphology of treated SSF is shown in Figures 3(b), 3(c), and 3(d). Because of the alkali treatment, these fibers have a typical rough surface topography. As illustrated in Fig. 3(b), this treatment has resulted in void formation and fiber fibrillation (fiber bundles fragmented into tiny fibers). This increases the effective surface area of the matrix that can be contacted. In other words, the removal of hemicellulose and lignin causes the alkali treatment to produce a rough surface topography. It improves the fiber's aspect ratio, resulting in greater fiber matrix interface adhesion and improved mechanical characteristics. Alkali treatment prior to DCP and silane treatment may break hydrogen bonding in cellulose hydroxyl groups of sisal fibers, resulting in lignin elimination and a more reactive fiber surface. In Figs. 3(c) and 3(d), sisal fiber treated with DCP and silane, respectively, the SSF reveals rough surfaces, voids, and cell (fibrillar) structure in a parallel pattern. The treated SSF microphotographs show that the chemical treatment permits good wetting and that the fiber surfaces are completely different from the untreated SSF. It's worth noting that the DCP and silane treatments don't form bundles around the microfibrils, whereas the peroxide treatment's major purpose is to graft polyolefins (mostly PE) onto the cellulose surface. The grafting reaction is commonly caused by peroxide produced by a free radical reaction [5,16]. The following is a description of the reaction between an EVA matrix and cellulose fiber:

$$R\,O - O\,R \rightarrow 2\,R\,O\bullet$$

$$R\,O\bullet + EVA - H \rightarrow R\,O\,H + EVA\bullet$$

$$R\,O\bullet + CELLULOSE \rightarrow R\,O\,H + CELLULOSE$$

$$EVA\bullet + CELLULOSE \rightarrow EVA\bullet - CELLULOSE$$

Natural fibers are known to contain bound moisture, which can hydrolize the coupling agent, which is commonly represented by the formula $YRSiX_3$ (where X is a hydrolizable alkoxy group, Y is a functional group, and R is a small aliphatic chain). The hydrolysis product, silanol, can form covalent or hydrogen bonds, enhancing interfacial adhesion at the fiber-matrix interface. Figure 4 depicts the various reaction processes. The hydrolysis stage is crucial because it regulates the amount of silanol formed, which impacts the amount of condensation and oligomerization. A ductile interface is established when a long siloxane chain is produced on the natural fiber, but excessive chain lengths can also increase the likelihood of crosslinking reactions, which can result in brittle interfaces [4]. Due to hydrophobicity on the surface, the coupling agents on the SSF lower moisture content via long chain hydrocarbon attachments. Furthermore, these coupling agents permeate the cell wall through surface pores and aggregate in the fibrillar areas, preventing moisture from entering the cell.

3.4 Tensile properties

Fibers in a composite material's principal function is to support the applied mechanical forces. The load is transferred from the matrix to the fiber in a composite through shear deformation of the matrix around the fiber [33]. The shear deformation is caused by the differences in mechanical characteristics of the composite's constituents. Because matrix molecules can be fixed to the fiber surface by chemical reaction or adsorption, the interface is an area at least several molecular layers thick and its properties are intermediate between those of the fiber and matrix phases [30]. These features have been demonstrated by chemical treatments on SSF. Figure 5 shows the relative tensile strength of EVA-SSF biocomposites with various chemical treatments and fiber loadings. Although some formulations did not demonstrate significant changes ($p>0.05$), biocomposites including treated SSF showed higher relative tensile strength than untreated fiber composites. The addition of untreated and treated SSF (at 10% wt.) to the matrix resulted in a significant loss in tensile strength. This is owing to the matrix's loss of mobility and discontinuity. The dilution of the fibers is spread as the fiber content is increased, resulting in a modest rise in characteristics. At a fiber concentration of 10% wt, biocomposites produced with alkali treatment outperform composites with untreated, DCP, and silane treated fibers in terms of tensile performance. The increased surface adhesive qualities (after removal of natural and artificial contaminants) causing a

rough surface topography are responsible for the improved tensile strength reported in biocomposites formed with alkali treated SSF. Silane treatment improves tensile strength significantly when the fiber content is high (20% wt.). The larger surface area associated with treated fibers produces more surface contact with the matrix, which could explain why biocomposites formed with treated SSF have better tensile strength qualities. With increased concentrations of SSF, the relative tensile modulus of the biocomposites reinforced with SSF (as shown in Fig. 6) increases. This is owing to the solid structure of particle SSF reinforcement, which gives the polymeric matrix more rigidity. When the fiber concentration of EVA-SSF biocomposites exceeded 20% wt, two distinct types of behavior were identified. The first was typical of composites reinforced with untreated and alkali-treated fibers, whereas the second was typical of DCP and silane-treated SSF composites. The relative tensile modulus of untreated and alkaline-treated SSF biocomposites evolves in two zones, as shown in Fig. 6, all of which are dependent on fiber content. The elastic modulus increases smoothly from 1 to 36.1 MPa for fiber content up to 20% wt, and we can assume that the tensile modulus rises at a consistent rate in this scenario. There is an increase up to maximum value for higher fiber content up to 30% wt (untreated and alkaline treated samples). After then, even for fiber concentrations of 40 percent wt, this characteristic tends to stabilize to similar values. Biocomposites reinforced with SSF and treated with DCP and silane, on the other hand, show consistent increases in tensile modulus, as illustrated in Fig. 6. In the current study, two factors influenced the increase in tensile modulus: fiber volume fraction and particular treatment, especially at fiber concentrations larger than 10% wt. At varying fiber loadings, Fig. 7 shows a constant decrease in relative elongation at break of composites as a function of fiber treatment. A decrease in the deformability of a hard interface between the fiber and matrix components could explain the lower elongation at break. Although all of the samples show a dramatic decline, there are some minor variances ($p<0.05$). This decrease shows that interfacial bonding levels are crucial. When the fiber concentration was greater than 10% by weight, however, there was no discernible change. Flexural tests (three and four point bending), interlaminar shear stress (ILSS), Iosupescu shear tests, single fiber pull out tests, and other techniques are used to characterize the fiber-matrix interface interface strength [33]. The stiffness and brittleness of the biocomposite gradually rise as the fiber content increases, resulting in a decrease in elongation. Increasing the fiber content in biocomposites causes a steady increase in stiffness and brittleness, as well as a decrease in elongation. Untreated fibers have a larger effect than those treated with DCP and silane coupling, according to current findings. Increasing the fiber composition of a composite results in considerable changes in its qualities, such as stiffness and brittleness. Although the hardness of the composites rises, both attributes are associated with a decrease in elongation of EVA-SSF biocomposites.

3.5 Fracture surfaces

The tensile fracture surfaces of composite samples made up of 30% wt untreated and treated SSF were studied using a scanning electron microscope (SEM). During stretching, the treated fibers stick effectively to the polymer matrix and break and delaminate (Figs. 8(b)-8(d)). Untreated sisal fibers, on the other hand, are almost intact when pulled out of the matrix, as seen in Fig. 8. (a). This indicates that the fiber and EVA matrix have inadequate interfacial adhesion, confirming the lack of physical contact between the components. The large contrast in character and surface energy between untreated SSF and the EVA matrix resulted in poor interfacial adhesion. A microphotograph of SSF after alkaline treatment is shown in Fig. 8(b). This treatment increased the adhesion between SSF and the EVA matrix. Figures 8(c) and 8(d) show microphotographs of SSF biocomposites treated to DCP and silane treatments, respectively. Such findings suggest that fiber aggregation into a bundle format is inhibited, implying that treated SSF interacts better with the EVA matrix than untreated SSF. Fiber pull-out and debonding have been minimized as a result of these treatments. From a micromechanical standpoint, improved adhesion at the fiber-matrix interface leads to a reduction in the critical fiber length for successful stress transfer. The interfacial interaction of the EVASSF biocomposites with treated SSF was superior. Poor mechanical characteristics can be caused by a lack of interfacial interaction, and the SEM tests back up the tensile results reported in the previous section.

4. Conclusions

The findings show that by altering the fiber surface, it is possible to improve the properties of EVA-SSF biocomposites by generating a suitable interface with the polymeric matrix. Chemical treatments alter the spectra and surface properties of SSF, according to FTIR investigations. The chemical treatments performed on SSF improved thermal stability and converted cellulose I to cellulose II. The quantity of cellulose in SSF is directly connected to the A_{1430}/A_{900} ratio. Composites reinforced with modified fibers exhibit better mechanical properties than those reinforced with untreated SSF, owing to increased fiber-matrix adhesion. Due to their rough surface topography and chemical connection between the fiber and the EVA matrix, silane treated fiber biocomposites had the best tensile characteristics compared to other treatments. Chemical treatments improve fiber-matrix adhesion, according to SEM microphotographs. The contact between the fiber and the matrix is substantially stronger when silane coupling agents are utilized, according to tensile failure surfaces created with treated fibers. The EVA-SSF biocomposites developed have a velvety, smooth look that resembles wood. As a result, this material might be utilized to replace wood in panels, covers, and a wide range of other applications.

Acknowledgments

Mr. Madera-Santana wants to thank to British Council for the grant awarded during his stay at Department of Materials (IPTME) of Loughborough University. (Grant Num. MEX-2900120).

Appendix A: Tables

Table 1. Physical properties of sisal fibers and ethylene vinyl acetate (EVA) copolymer.

Property	Values
Short sisal fiber Fiber diameter, □m	80-290
Density, g/cm^3	1.48
Pectin content, %	1.5-2
Lignin content, %	3.6-5.7
Hemicellulose content, %	10.3-17.8
Cellulose content, %	77-87
Tensile strength, MPa	410-720
Tensile modulus, GPa	8.5-18.4
Elongation at break, %	4.5-13.2
EVA matrix [a]	
Melt flow index	5.4
Tensile strength, MPa	10.4
Tensile modulus, MPa	80.9
Elongation at break, %	> 700

Table 2. Relative absorbance of SSF at different chemical treatments

Treatment	$A_{4000-2995}/A_{1337}$	A_{1430}/A_{900}
Untreated	0.9465	1.0683
Alkaline	0.9255	0.9795
DCP	0.9145	0.9683
Silane	0.9248	1.0463

Appendix B: Figures

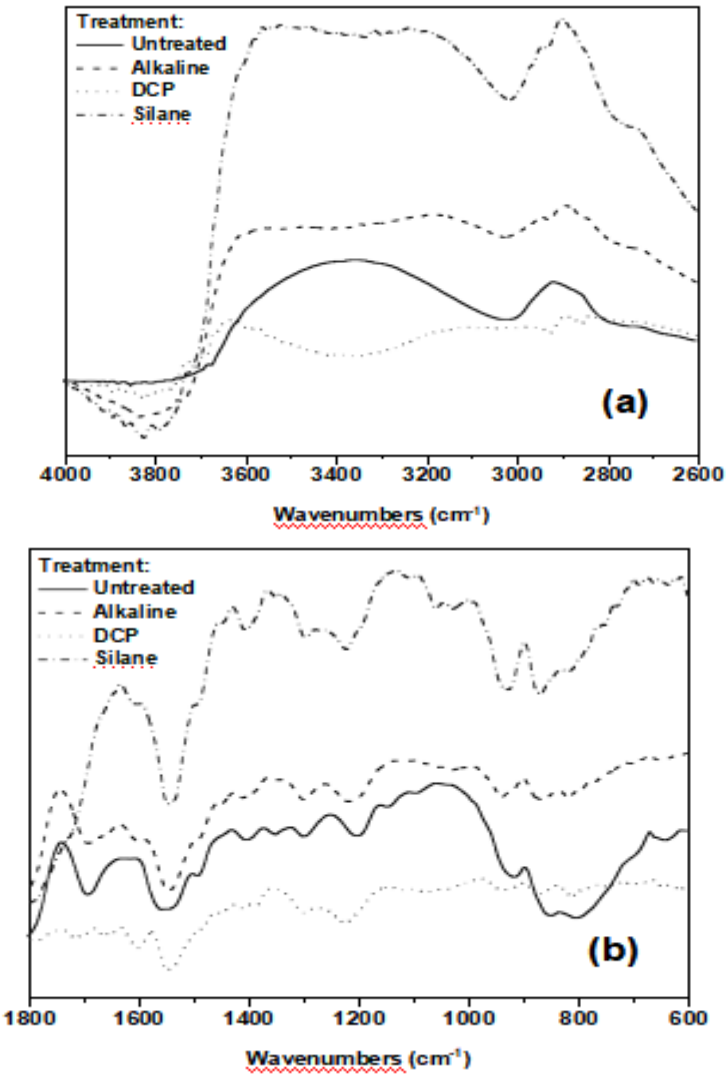

Fig. 1. Infrared spectra of SSF treated and untreated, (a) at 4000-2600 cm^{-1} and (b) at 1800-800 cm^{-1}.

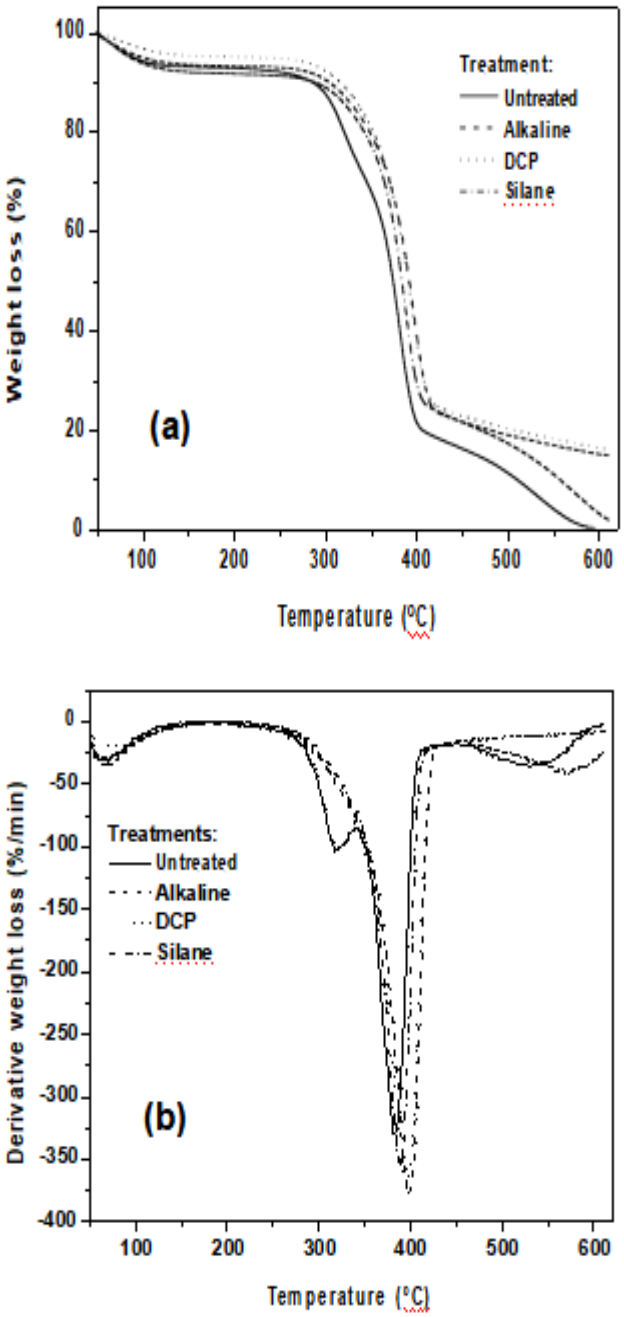

Fig. 2. Effect of fiber treatment on weight loss (a) and on derivative weight loss (b), as function of temperature.

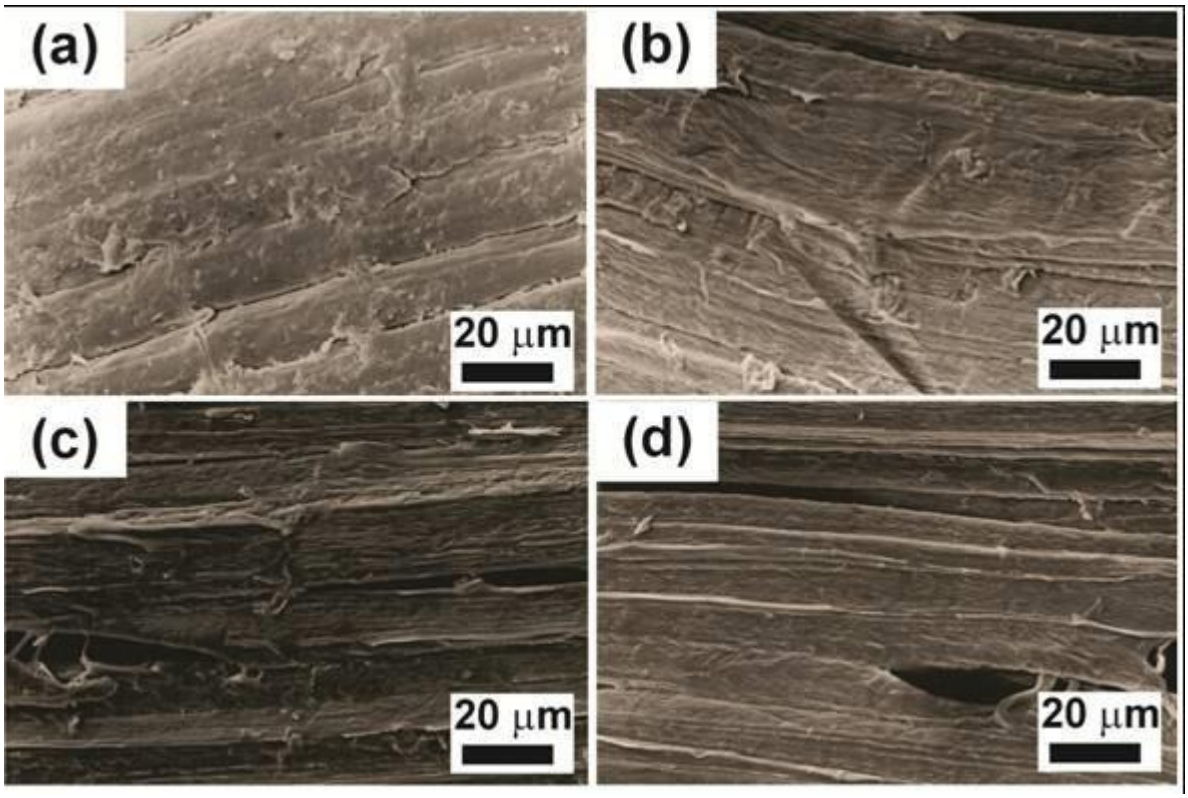

Fig.3. Scanning electron microphotographs of SSF, (a) untreated, (b) alkaline, (c) DCP and (d) silane treatment.

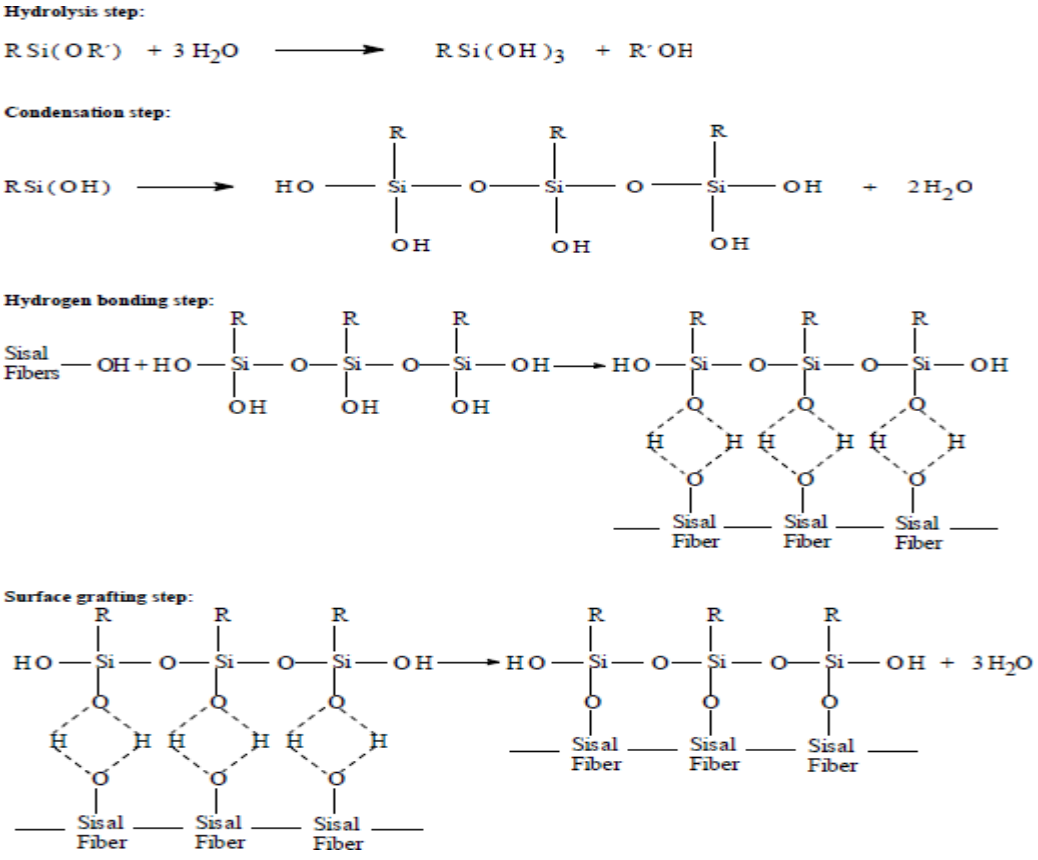

Fig. 4. Reaction of silane grafting on natural fibers [4].

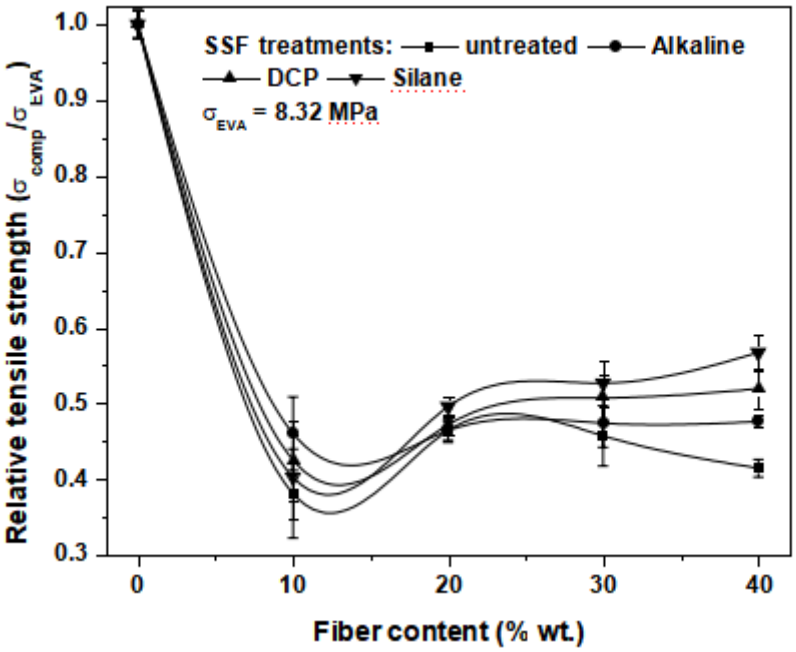

Fig. 5. Relative tensile strength of the EVA-SSF biocomposites.

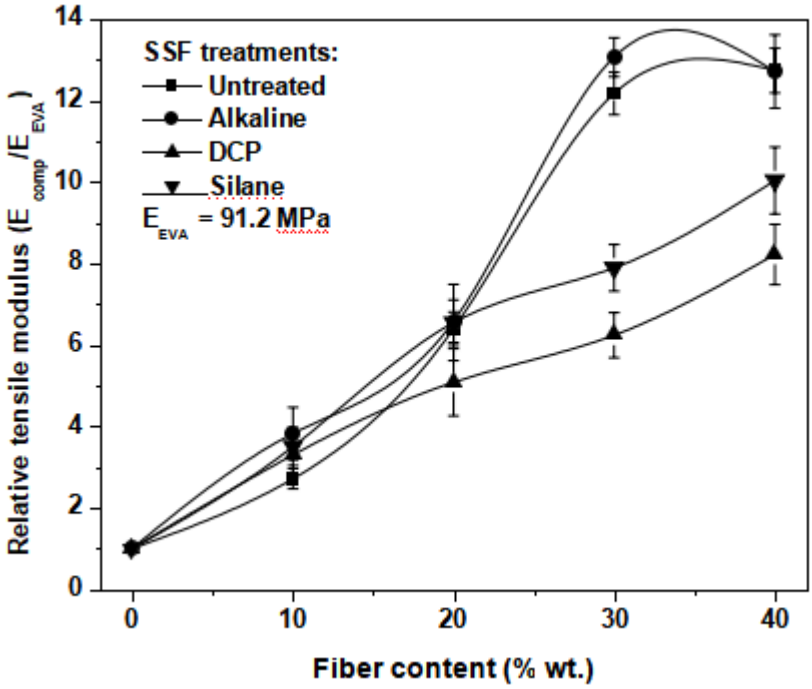

Fig. 6. Relative tensile modulus of the EVA-SSF biocomposites.

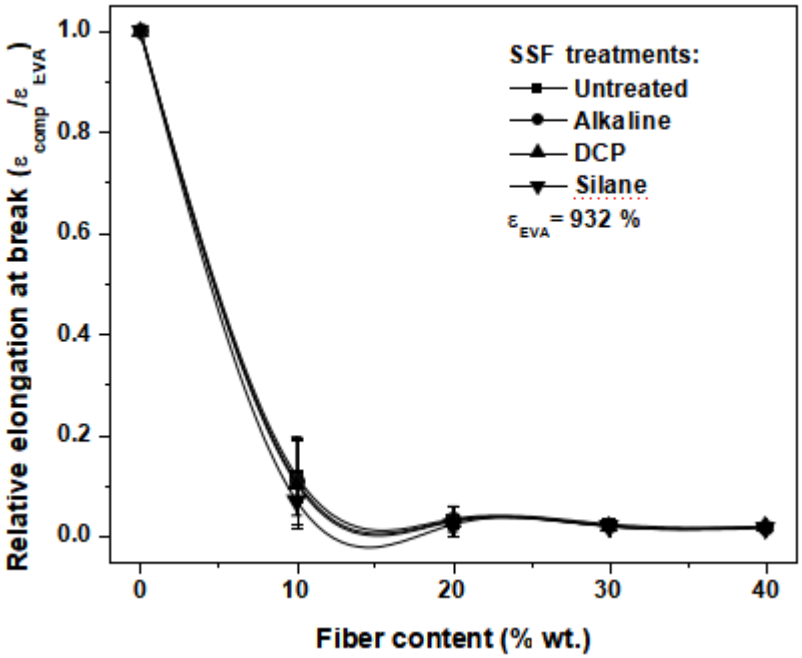

Fig. 7. Relative elongation at break of the EVA-SSF biocomposites.

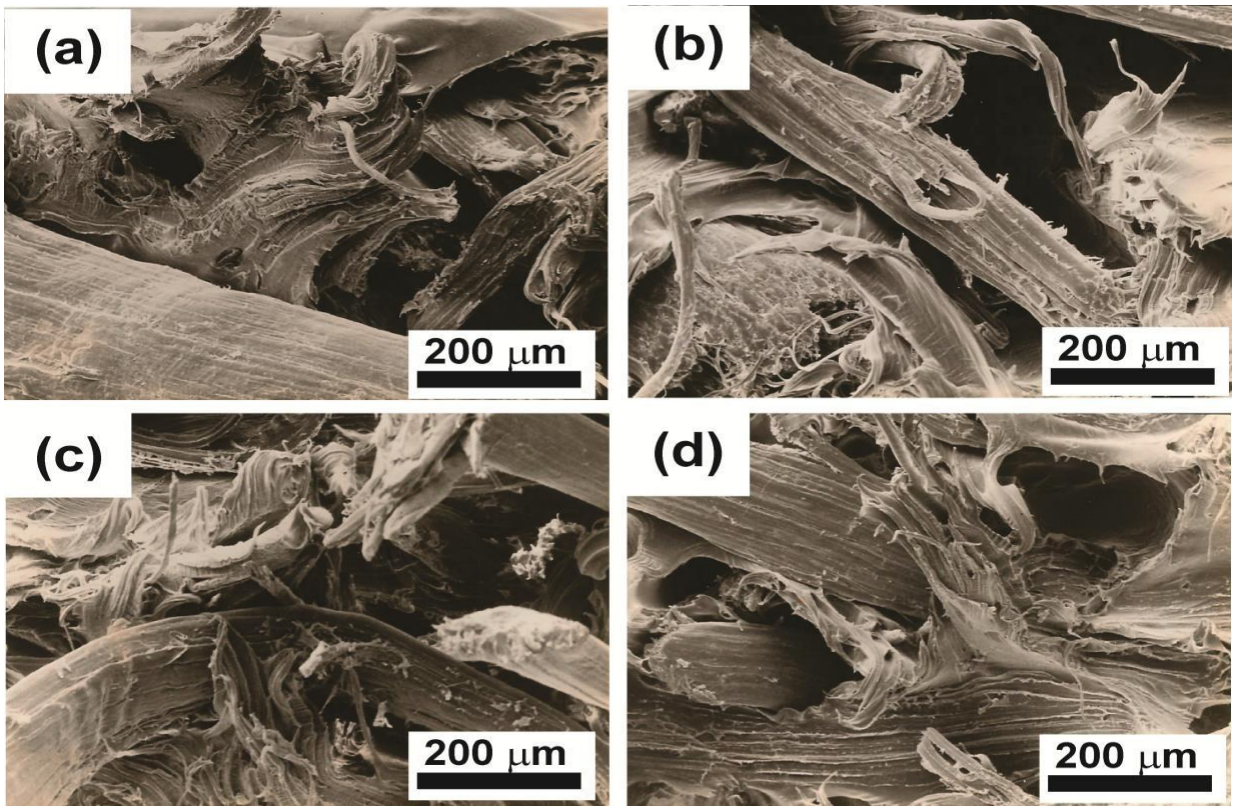

Fig. 8. Scanning electron microphotographs of the tensile surface of 30% wt. SSF-EVA biocomposites: (a) untreated, (b) with alkaline treatment, (c) with DCP treatment and (d) with silane treatment.

References

[1] . V.G. Geethamma, K. Thomas, R. Lakshminarayanan, and S. Thomas, S., *Polymer*, 36, 1483 (1988).
[2]. J. George, J., S. Bhagawan, N. Prabhakaran, and S. Thomas, S., *J. Appl. Polym. Sci*., 57, 843 (1995).
[3]. K. Joseph, S. Thomas, C. Pavthran, and M. Brahmakumar, M., *J. Appl. Polym. Sci*., 47, 1731 (1993).
[4]. R. Karnani, M. Krishnan, and R. Narayan, R., *Polym. Eng. Sci*., 37, 476 (1997).
[5]. X. Li, L.G. Tabil, and S. Panigrahi, *J. Polym. Environ*., 15, 25 (2007).
[6]. S. Kalia, B.S. Kaith, and I Kaur, *Polym. Eng. Sci*., 49, 1253, (2009).
[7]. L.Y. Mwaikambo, and M.P. Ansell, *J. Appl. Polym. Sci.*, 84, 2222 (2002).
[8]. E.T.N. Bisanda, and M.P. Ansell, *Comp. Sci. Technol*., 41, 165, (1991).
[9]. Y. Mwaikambo, and M.P. Ansell, *Angew. Makromol*., 272, 108 (1999).
[10]. D. Nabi Saheb, and J.P. Jog, *Adv. Polym. Technol*., 18, 351 (1999).
[11]. S. Th. Georgopoulos, P.A. Tarantili, E. Avgerinos, A.G. Andreopoulos, and E.G. Koukios, *Polym. Deg. Stabil*., 90, 303 (2005).
[12]. L.H. Lee, *Polym. Eng. Sci*., 9, 213 (1969).
[13]. G. Kalaprasad, K. Joseph, S. Thomas, and C. Pavithran, *J. Mat. Sci*., 32, 4261 (1997).
[14]. M.J. John, and R.D. Anandjiwala, *Polym. Comp.*, 29, 187 (2008).
[15]. J. Chang Do. US Patent 2008/0145656 A1.
[16]. K. Joseph, S. Thomas, and C. Pavithran, *Polymer*, **37**, 5139 (1996).
[17]. A. Alvarez Vera, and A Vazquez, *Composites Part A*, **37**, 1672 (2006).
[18]. J. Gassan, and A.K. Bledzki, *Composites Part A*, **28a**, 1001 (1997).
[19]. A.M. Mohd Edeerozey, and H.Md. Akil, *Mater. Lett*., **61**, 2023 (2007).20
[20]. M.A. Henderson, *IEEE Electr. Insul. Mat*., **9**, 30 (1993).
[21]. D.G. Dikobe, and A.S. Luyt, *Expr. Polym Lett*. **3**, 190 (2009).
[22]. M.A. Mydul, T. Ahmet, M.M. Haque, M.A. Gafur, and H.A.N.M. Kabir, *Polym. Plast. Technol. Eng*., **48**, 110 (2009).
[23]. M.E. Malunka, A.S. Luyt, and H. Krump, *J. Appl. Polym. Sci*., **100**, 1607 (2006).
[24]. A. Espert, F. Vilaplana, and S. Karlsson, *Composites Part A*, **35**, 1267 (2004).
[25]. C.A. Cruz-Ramos, in "Mechanical Properties of Reinforced Thermoplastics". Clegg, D.W. and Collyer, A.A., Eds., Chap. **3**, Elsevier Applied Science Publishers, London, (1986).
[26]. P.A. Sreekumar, J. Kuruvilla, G. Unnikrishnan, and S. Thomas, *Polym. Eng. Sci*., **32**, 131 (2011).
[27]. M.L. Nelson, and R.T. O´Connor, *J. Appl. Polym. Sci*., **8**, 1311 (1964).
[28]. S.S. Reedy, *J. Appl. Polym. Sci*., **41**, 2363 (1990).
[29]. S.Y. Oh, D. Yoa, Y. Shinb, and G. Seoc, *Carbohydr. Res*., **340**, 417 (2005).
[30]. P.J. Herrera-Franco, and A. Valdez-Gonzalez, in "Natural Fibers, biopolymers and biocomposites", A.K. Mohanty, M. Misra and L.T. Drzal Eds. Chap. **6**, CRC Press, USA, (2005).
[31]. F. Yao, Q. Wu, Y. Lei, W.Guo, and Y. Xu, *Polym. Deg. Stabil.*, **93**, 90 (2008).
[32]. P. Gañan, and I. Mondragon, *Polym. Comp*., **90**, 303 (2002).
[33]. R.P. Sheldon, in "Composite Polymeric Materials". Elsevier Applied Science Publisher, London, (1982).

Alhassani A. H received the bachelor's degree from the University of Basra, Basrah, Iraq, the master's degree from the University of Bradford, Bradford, U.K., and the Ph.D. degree from Loughborough University, Loughborough, U.K.,He is currently the General Director of the Basra Centre for Strategic Studies and also the Chancellor of the Iraq University College Basrah, Basrah. His research interests include environmental monitoring and applications in construction and disaster prevention.

DOI: yy.yyyy/IUCJEAS., 2022vol 2., issue.1

مجلة كلية العراق الجامعة للهندسة والعلوم التطبيقية

الخصائص الفيزيائية والكيميائية لألياف السيزال القصيرة ومركبات الأثيلين فينيل أسيتات بعد معالجة الألياف السطحية

عبد الهادي الحساني[1]،
1 كلية العراق الجامعة – قسم هندسة الاتصالات – البصرة – العراق
البريد الالكتروني : alhassani@yahoo.com[1]

الملخص. الالياف الطبيعية هي مورد رخيص وسهل التجديد لمركبات البوليمر الغنية بالسليلوز. من ناحية أخرى ، تقلل الـ شوائب (الشموع ، اللجنين ، إلخ) ومجموعات الهيدروكسيل من احتمالية تعزيز مصفوفات البوليمر NF .تم تطبيق ثلاث معا لجات كيميائية مختلفة على ألياف السيزال القصيرة (بيروكسيد ديكوميل ، قلوي وسيلاني). تم استخدام الخلط الميكانيكي في مـ رحلة الذوبان في مصفوفة البوليمر (130oC) لإنشاء مركبات من أسيتات فينيل الإيثيلين (EVA) و SSF المعدل كيميائياً. تمت دراسة الخواص الميكانيكية للمركبات الحيوية فيما يتعلق بمحتوى الألياف والمعالجة الكيميائية. كان لكل مركب مقوى من SSF تم معالجته قوة شد أعلى. زاد مركب معامل المرونة زيادة كبيرة عند مقارنته بالمصفوفة الفارغة. مع ارتفاع محتو ى الألياف ، انخفض الاستطالة عند قيم القطع . علاوة على ذلك ، تم اكتشاف أن المعالجة السطحية لـ SSF زادت من تشتت ا لألياف داخل مصفوفة EVA . تم استخدام التحليل الحراري الوزني (TGA) لفحص الاستقرار الحراري لـ SSF . نظرًا لأ ن الألياف الطبيعية لها ثقل نوعي أقل ، فهي أقل تكلفة ولها فائدة إضافية تتمثل في قابلية التحلل البيولوجي ويمكن أن تكون إع ادة تدوير المواد المركبة.